Published in final edited form as:
Vet Radiol Ultrasound. 2012 ; 53(4): 474–481. doi:10.1111/j.1740-8261.2012.01947.x.

HELICAL TOMOTHERAPY SETUP VARIATIONS IN CANINE NASAL TUMOR PATIENTS IMMOBILIZED WITH A BITE BLOCK

Lyndsay N. Kubicek, **Songwon Seo**, **Richard J. Chappell**, **Robert Jeraj**, and **Lisa J. Forrest**
Department of Surgical Sciences (Kubicek), School of Public Health, Department of Biostatistics and Medical Informatics (Seo, Chappell), and Surgical Science (Jeraj, Forrest), University of Wisconsin

Abstract

The purpose of our study was to compare setup variation in four degrees of freedom (vertical, longitudinal, lateral, and roll) between canine nasal tumor patients immobilized with a mattress and bite block, versus a mattress alone. Our secondary aim was to define a clinical target volume (CTV) to planning target volume (PTV) expansion margin based on our mean systematic error values associated with nasal tumor patients immobilized by a mattress and bite block. We evaluated six parameters for setup corrections: systematic error, random error, patient–patient variation in systematic errors, the magnitude of patient-specific random errors (root mean square [RMS]), distance error, and the variation of setup corrections from zero shift. The variations in all parameters were statistically smaller in the group immobilized by a mattress and bite block. The mean setup corrections in the mattress and bite block group ranged from 0.91 mm to 1.59 mm for the translational errors and 0.5°. Although most veterinary radiation facilities do not have access to Image-guided radiotherapy (IGRT), we identified a need for more rigid fixation, established the value of adding IGRT to veterinary radiation therapy, and define the CTV–PTV setup error margin for canine nasal tumor patients immobilized in a mattress and bite block.

Keywords

canine nasal tumor; helical tomotherapy; radiation therapy; setup variations

Introduction

Intensity-modulated radiation therapy (IMRT) produces precise dose distributions that conform tightly to targets and decrease high doses to normal structures through the generation of steep dose gradients. IMRT aims at increasing the therapeutic index by maximizing tumor control probability (TCP) while minimizing normal tissue complication probabilities (NTCP).To increase therapeutic index, higher conformity is being achieved with reductions in planning target volume (PTV) margins. The PTV margin is typically obtained by adding a predetermined symmetric margin to the clinical target volume (CTV). The CTV is defined as the microscopic expansions of the gross tumor volume (GTV). The PTV margin encompasses patient setup errors (systematic and random errors) and other uncertainties such as movement, and is dependent on the type of immobilization devices employed.

Image-guided radiotherapy (IGRT) uses online imaging prior to treatment delivery to improve the likelihood that radiation is delivered as closely as possible to the original plan.[1]

Address correspondence and reprint requests to Lyndsay Nichole Kubicek at the above address. lbunting@svm.vetmed.wisc.edu.

As treatment plans increase in complexity, the resulting dose delivery must be concise to avoid unrecognized geographic misses that may result in tumor recurrence and/or radiation toxicity. Systems in use in people for image guidance include port films, electronic portal imaging, fluoroscopic imaging, ultrasound, implanted fiducial-based tracking systems, and helical and cone beam CT.[2] The aforementioned imaging modalities have the ability to be used in veterinary medicine when available. Previous studies in veterinary medicine have evaluated the use of a thermoplastic mask alone, and in conjunction with a support bridge, dental mold, and deformable neck bridge.[3, 4] IGRT, a feature of Helical Tomotherapy, provides the ability to evaluate patient setup in six degrees of freedom: lateral, longitudinal, vertical, pitch, yaw, and roll. Pitch, roll, and yaw are parameters of angles of rotation in three dimensions around a defined line, in this case the line parallel to the couch. Pitch is an up-down rotation, yaw is a left-right rotation, and roll is a rotation along this line. Pitch and yaw can not be corrected because the couch does not move in this direction. Because tomotherapy treats in a helical fashion, roll can be adjusted.

Compared to other regions, tumors of the head and neck tend to have less inherent mobility due to their attachment to underlying bone.[5] Normal structures in close proximity to nasal tumors are the eyes, cribriform plate and brain, and hard palate. The expansion of the CTV into the PTV may overlap with the normal regions at risk depending on immobilization devices used. Setup variations have been examined in animals undergoing radiation therapy using multiple immobilization techniques such as deformable mattresses, bite blocks, and thermoplast masks.[6–8] Limited data are available regarding the evaluation of setup variation for patients undergoing radiation therapy in more than three degrees of freedom (lateral, longitudinal, and vertical).

Our primary goal was to compare setup variation in four degrees of freedom (vertical, longitudinal, lateral, and roll) between canine nasal tumor patients immobilized with a mattress* and bite block†, and a mattress* alone. Our secondary goal is to define a CTV to PTV expansion margin based on our mean systematic error values for canine patients with head and neck tumors immobilized by a mattress* and bite block.†

Materials and Methods

We evaluated dogs treated with helical tomotherapy, either immobilized by a vacuum deformable mattress* alone (Group 1) or a vacuum deformable mattress* and bite block† (Group 2). Between January 2003 and September 2006, 31 dogs with a biopsy-confirmed sinonasal tumor were treated with helical tomotherapy in the context of a phase I/II fixed dose clinical trial of conformal avoidance (Group 1).[9] Fifteen of the 31 dogs had complete registration data available for analysis. Between August 2009 and the present, 18 client-owned dogs with biopsy-confirmed sinonasal tumors have been enrolled and treated with helical tomotherapy in a current phase I/II canine dose painting study (Group 2). Fifteen of the 18 patients have complete registration data available for analysis. Eighteen of 18 patients have translational data available (lateral, longitudinal, vertical).

Patients in Group 1 were in sternal recumbency with the head and thorax immobilized in a deflatable Vac-Lok™ mattress* conformed to the body contour of the dog. Patients in Group 2 were set up in the same manner; however, their head was immobilized in a bite block. The bite block system involved the use of a plexiglass base in which an individualized dental mold was encased. Dental mold impressions were made using Dental

*Vac-Lok™ CIVCO, Orange City IA.
†3M-Express STD Putty™ 3M ESPE Dental Products, St. Paul MN.

3M-Express STD Putty™† The base of the bite block system was fixed to the CT and treatment couch by an indexing bar (Photograph 1).

Patients in Group 2 were anesthetized and positioned using their customized bite block dental mold and mattress. Helical megavoltage CT (MCVT) images were obtained with the tomotherapy unit using 2–3cGy imaging dose just before each daily treatment in real time.[10] Available MCVT slice thickness ranged from fine (2 mm), normal (4 mm), and course (6 mm), and were determined by the user, with normal the most commonly used slice thickness. Lengths of MVCT images in the rostral-caudal direction were chosen by the user and included the entire target and anatomic landmarks as needed. Planning CT to MVCT registration was performed initially by using an automatic process and then checked manually and adjusted if necessary before treatment. Group 1 patients were anesthetized and positioned in their customized immobilization mattress. Pitch and yaw could not be corrected automatically by couch movements in either group and were evaluated by the clinician and patients were rescanned under clinician judgment when the pitch and yaw were greater than 3.0° and could not be corrected with rotational, lateral, vertical, or longitudinal adjustments.

Group 1 patients were repositioned based on image alignment, in the lateral, longitudinal, vertical, pitch, roll, and yaw dimensions after final registration of the images. Later upgrades to the software automatically applied roll shifts. Shifts of 1 mm or greater were applied without reimaging, however, significant shifts (greater 3° roll, pitch, and yaw values that were not correctable through changes in the vertical or lateral adjustments), required a second MVCT after repositioning to ensure accurate delivery.[9]

Group 2 patient shifts in the vertical, longitudinal, and roll dimensions were applied automatically by couch shifts and gantry start position, and lateral shifts were done manually. Pitch and yaw rotations were not used, as they can not be corrected without physically moving the patient, thus only lateral, longitudinal, vertical, and roll shifts were corrected and used in this study.

Setup correction data were collected at time of MVCT scan for both groups. The first three patients in Group 2 did not have roll corrections entered if the roll was less than 0.5°; subsequent patients had roll corrections entered.

Data analysis consisted of overall distributions of setup corrections, patient-specific distributions of setup errors, and the distance errors of patient setup. The magnitude of patient-specific distributions were calculated in lateral, longitudinal, vertical, and roll directions. Overall distributions of setup corrections, which groups together with all fractions for all patients, were plotted to assess ranges of corrections that were made in different directions. Distributions of patient-specific setup errors were quantified to assess systematic and random components of setup corrections and patient–patient variation.

A four-parameter model was used to analyze the setup error of a patient population, with each individual patient having their own setup error.[11, 12] The four-parameter model is used to separate the total distribution of positioning corrections into a distribution of patient-specific random setup errors and a distribution of patient-specific systematic errors. Systematic error can be defined as the mean (μ_i) of positioning corrections for the patient, and the random error can be defined as the standard deviation (σ_i).[11]

In this study, we assessed six parameters for setup corrections: (1) systematic error, (2) random error, (3) patient–patient variation in systematic errors, (4) magnitude of patient-specific random errors (root mean square [RMS] of the random errors), (5) distance error, and (6) variation of setup corrections from zero shift.

Individual systematic error was defined as the mean of setup corrections for individual patient.

Individual systematic error (μ_i) is given by equation 1[2, 12]:

$$\mu_i = \sum_{K=1}^{Ni} \frac{m_k}{N_i}, \quad (1)$$

where N_i is the number of fractions for patient i, and m_k is the measured positioning setup correction for the k^{th} fraction for patient i. Individual random error was defined as the standard deviation of setup corrections for individual patient.

Individual random error (σ_i) is given by equation 2[2, 12]:

$$\sigma_i = \sqrt{\frac{\sum_{K=1}^{Ni} (m_k - \mu_i)^2}{(Ni - 1)}}, \quad (2)$$

where N_i is the number of fractions for patient i, m_k is the setup correction, and μ_i is the systematic error for patient i.

Variation in systematic errors is given by equation 3[2, 12]:

$$\sum(\mu_i) = \sqrt{\frac{\sum_{i=1}^{p} N_i(\mu_i - M(\mu_i))^2}{(N-1)}} \text{ where} M(\mu_i) = \sum_{i=1}^{p} \frac{N_i \mu_i}{N}, \quad (3)$$

where N is defined as the total number of fractions, and M(μ_i) is defined as the overall systemic error.

RMS (σ_i) is the RMS of the random errors, which is defined as the magnitude of random errors and is given by equation 4[2, 12]:

$$RMS(\sigma_i) = \sqrt{\sum_{i=1}^{p} \frac{(N_i - 1)(\sigma_i)^2}{(N-1)}} \quad (4)$$

The systematic errors in Table 1 using equation 1 might be underestimated in terms of the magnitude of setup corrections (i.e., distance from zero shift) since there is a tradeoff between setup corrections with different directions (+ or −). In Table 4, absolute values of setup corrections were used to examine the distribution of setup corrections regardless of directions of errors (named “distance error” in this study). Individual distance error was defined as the mean of absolute values of setup corrections for individual patient and was calculated using equation 5:

Individual distance error (DE_i)

$$DE_i = \sum_{K=1}^{Ni} \frac{|m_k|}{N_i} \quad (5)$$

Individual random error in equation 2 was defined as the standard deviation of setup corrections for individual patients. However, this measurement may have a limitation in assessing the variation of setup corrections from the setup shift of zero because the measurement used an average value of setup corrections for each patient as a baseline point for the variance instead of the zero shift. Individual variation of setup corrections was defined as the standard deviation from the setup shift of zero for individual patient and was calculated using equation 6:

Variation of setup corrections from the zero shift (VE_i)

$$VE_i = \sqrt{\frac{\sum_{K=1}^{Ni} (m_k - 0)^2}{Ni}} \quad (6)$$

Wilcoxon rank sum test was used for the comparison of each parameter for setup corrections between the two groups (Group 1 vs. Group 2). Statistical analysis was performed with SAS 9.2‡, and a *P*-value of <0.05 was considered statistically significant.

Results

The mean setup correction for each individual patient in the translational (lateral, longitudinal, vertical) and rotation directions is in Fig. 1. These figures provide a graphical indication of the setup behavior of each patient during the course of radiation therapy. The interpatient and intrapatient variation for Group 2 patients was smaller than for Group 1 patients. Tables 1 and 2 show the comparison of the systematic and random errors between the two groups, respectively. The systematic error can be defined as the reproducible inaccuracies that are constantly in the same direction. Random error can be defined as fluctuations in the measured data due to the precision limitations of the measurement device, and are inherently unpredictable.

Based on the translational coordinates, directions were either positive or negative, and thus the systematic error in Table 1 might be underestimated in terms of the magnitude of setup corrections (i.e., distance from zero shift), and thus the distance errors (equation 5 was used in Table 4 to assess the setup corrections in terms of the distance of the errors from zero shift.

Figure 2 shows the graphical results of Table 3, which is the variation in systematic errors and magnitude of random errors for each group. The variation in systemic errors describes a variation between patients, and the magnitude of random error describes an overall variation within the subset of patients. The variations in systemic error for translational and rotational directions range from 0.58 mm to 1.23 mm and 0.57° in Group 2 patients, and 1.68 mm to 2.05 mm and 2.01° in Group 1 patients. The magnitude of random errors range from 1.14 mm to 1.86 mm and 0.74° in Group 2 patients and 2.99 mm to 3.12 mm and 2.29° in Group 1 patient population. The distance errors of the setup corrections for the translational and rotation directions are presented in Table 4. The mean setup corrections in the Group 2 ranged from 0.91 mm to 1.59 mm for the translational errors and 0.5° for the rotation error, and 2.38 mm to 2.68 mm for the translational errors and 2.15° for the rotation error in Group 1 patients, which is statistically significant in all directions between the two groups.

‡SAS 9.2 Software Cary, NC.

The individual random error in Table 2 is defined as the standard deviation of setup corrections for individual patients. Due to limitation of the random error in assessing the variation of setup corrections from the zero shift, the variation from the zero shift was calculated from a baseline of zero (Table 5). The mean of the variations of setup corrections in Group 2 ranged from 1.7 mm to 1.85 mm for translational errors and 0.7° for rotational error; 2.91 mm to 3.26 mm for translational errors and 2.67° for rotational error in Group1 and are statistically significant in all directions between the two groups.

The mean distance errors reported in Table 4 for Group 2 were used to define the CTV to PTV expansion. The absolute values were used to reduce underestimations in the magnitude of setup corrections. The mean setup corrections in the Group 2 ranged from 0.91 mm to 1.59 mm for the translational errors and 0.5° for the rotation error.

Discussion

The PTV margin is a geometric concept that accounts for intrafraction motion, interfraction motion, and setup uncertainties. ICRU report 62 segments the PTV into two distinct submargins; one termed the setup margin (SM), which accounts for uncertainties associated with patient setup and the other, the internal margin, which accounts for target motion.[13, 14] Proper immobilization in combination with volumetric image guidance can reduce the uncertainties in the SM, interfractional, and intrafractional motion.

Impact of setup uncertainty has been investigated by several authors involving immobilization and localization techniques in human head and neck IMRT.[15–18] Clinical consequences of setup uncertainty in veterinary medicine are limited. Two recent studies have been performed evaluating various immobilization techniques.[3, 4] The first study evaluated systematic and random setup errors associated with the use of an immobilization device comprised of a custom made support bridge, bite block, vacuum-based foam mold, and a modified thermoplastic mask attached to a commercially available head rest, concluding a 2 mm CTV–PTV expansion was appropriate when using a kilovoltage onboard imaging system.[3] The later mentioned study evaluated a thermoplastic mask alone, with orthogonal 2-dimensional digitally reconstructed images concluding a 3–6 mm CTV–PTV expansion was appropriate. However, this study only evaluated the three Cartesian planes (vertical, longitudinal, and lateral).[4] A virtual planning study was performed evaluating the impact of daily setup variation on optimized IMRT canine nasal tumors plans when variations were not accounted for due to lack of image guidance. There was a loss of equivalent uniform dose (EUD) for target volumes of up to 5.6%, which corresponded to a potential loss in tumor control probability (TCP) of 39.5%. Overdosing of eyes and brain was noted by increases in mean normalized total dose (NTD_{mean}) and highest normalized dose given to 2% of the volume ($NTD_{2\%}$), concluding the successful implementation of canine nasal IMRT requires daily image guidance to ensure accurate delivery of precise IMRT distributions when non-rigid immobilization techniques are employed.[19]

In the study reported herein, patients immobilized with a mattress and bite block had longitudinal shifts affected mostly by the use of the indexing bar (Fig. 1). The indexing bar also reduced the potential influence of yaw dimension. Patients within Group 1 did not have a bite block and indexing bar, and marks on the immobilization mattress and the right maxillary canine tooth were used for laser alignment.

When evaluating mean setup corrections and error bars for translational and rotational directions, the last five patients in Group 2 had larger variation in their corrections. The first 13 patients were imaged initially and set up by the same people involved in the daily setups whereas the remaining five were imaged initially and setup for the planning CT by one

group and setup for daily treatment by another group. This demonstrates the need for consistency in patient initial setup for the planning CT (analogous to a CT simulation in human medicine) and daily treatment setup, in particular the creation of the dental mold. The advent of the dental mold and bite block reduce the roll corrections (Fig. 1) between the two groups, reported herein.

Although the corrections in the lateral direction are smaller for Group 2 compared to Group 1, the lateral corrections have larger variations compared to the roll corrections; intuitively one would think the bite block would reduce such variation. The lateral direction is influenced partly by yaw. Body yaw may be reduced by the indexing bar, but there may be yaw present in the head if the dental mold loses rigidity. This may occur over time, as the mold is used repeatedly over weeks, or more likely, if the premolar and molar teeth are not seated deeply within the mold material. This emphasizes the need to ensure all teeth are well covered by the dental material, not just relying on the purchase of the canines and incisors.

The use of a bite block and dental mold† may raise the concerns of photon beam attenuation. Tomotherapy treatment planning systems§ used a superposition/convolution algorithm. Superposition/convolution considers primary and scattered radiation separately and also scales the scatter kernel obtained with respect to the inhomogenities that surround it. Thus, superposition/convolution is less affected by tissue inhomogenities compared to previously used pencil beam algorithms. Regardless of photon beam algorithm, the treatment planning system should be able to use the Hounsfield units from the planning CT. The mean Hounsfield measurements for the dental mold† and bite block are 1109HU and 65HU, respectively, both of which are encompassed in our image-value-to-density table (IVDT), The CT simulation should include all aspects of the patient and setup for accurate dose distribution calculations. The CT simulation of all patients is done with patient-specific dental mold and bite block, thereby accounting for CT attenuation of these structures. Furthermore, delivery quality assurance is performed on all patients prior to dose delivery, ensuring appropriate, and safe delivery.

The potential bolus effect of the dental material† on the oral gingival and bite block on the buccal surface pose a concern. Data previously evaluated (not shown) did not show an increase in oral mucositis toxicity grading compared to patients without a dental mold and bite block.[20] As mucositis is an acute effect and rarely a dose limiting toxicity, we did not find this potential disadvantage to outweigh the benefits of improved immobilization. An added advantage of tomotherapy is that the beams are directed in all directions so that the dose is more uniformly distributed, which also abrogates such concerns.

We have shown that conventional mattress immobilization and laser alignment in combination with a bite block will provide reproducible and accurate positioning in canine sinonasal tumors. The mean positional offset for canine sinonasal tumors has been reported previously to range from 0.5 mm to 9.5 mm depending on the type of immobilization and image guidance used.[21] Our data fall within this range, with 0.91–1.59 mm for Group 2 patients compared to 2.38–2.68 mm for Group 1. Our two groups had the benefit of volumetric imaging, which allows for evaluation of all six degrees, i.e. three dimensions, of movement compared to orthogonal port films, which can only evaluate three dimensions.

The secondary goal was to propose a CTV–PTV expansion margin to account for setup uncertainties in patients immobilized with a mattress and bite block. In our study, most data fell within a shift of 2–3 mm in all the directions (Fig. 3). The mean distance error in the lateral direction was 1.35 mm, 0.91 mm in the longitudinal direction, and 1.59 mm in the

§TomoTherapy Inc., Madison, WI.

vertical axis, all of which would be encompassed in a 2 mm expansion, which was used in Group 2 patients. The PTV margin is obtained typically by adding a predetermined symmetric margin to the CTV. Previously reported data may lead to the suggestion of asymmetric expansion, in particular, limited in the lateral margins to aid in ocular avoidance. This is an area, in which there is limited data for and future dosimetric and clinical outcome studies would be needed.

Although most veterinary radiation facilities do not have access to IGRT, our data support the need for more rigid fixation, the addition of IGRT to veterinary radiation therapy, and defines the CTV–PTV setup error margin for canine head and neck patients immobilized in a mattress and bite block.

Acknowledgments

The authors would like to thank Michael Deveau, Stephen R Bowen, Ngoneh Jallow, and Matthew LaFontaine. This study was supported by RO1 CA136927.

REFERENCES

1. Dawson LA, Jaffray DA. Advances in image-guided radiation therapy. J Clin Oncol. 2007; 25:938–946. [PubMed: 17350942]
2. Schubert LK, Westerly DC, Tome WA, et al. A comprehensive assessment by tumor site of patient setup using daily MVCT imaging from more than 3,800 helical tomotherapy treatments. Int J Radiation Oncology Biol Phys. 2009; 73:1260–1269.
3. Harmon J, Van Ufflen D, LaRue S. Assessment of a radiotherapy patient cranial immobilization device using daily on-board kilovoltage imaging. Vet Radiol Ultrasound. 2009; 50:230–234. [PubMed: 19400474]
4. Kent MS, Gordon IK, Benavides I. Assessment of the accuracy and precision of a patient immobilization device for radiation therapy in canine head and neck tumors. Vet Radiol Ultrasound. 2009; 50:550–554. [PubMed: 19788043]
5. Eishruch A. Intensity-modulated radiotherapy of head-and-neck cancer: encouraging early results. Int J Radiat Oncol Biol Phys. 2002; 53:1–3. [PubMed: 12007933]
6. Kippenes H, et al. Comparison of the accuracy of positioning devices for radiation therapy of canine and feline head tumors. Vet Radiol Ultrasound. 2000; 41:1–376.
7. Green EM, Forrest LJ, Adams WM. A vacuum-formable mattress for veterinary radiotherapy positioning: comparison with conventional methods. Vet Radiol Ultrasound. 2003; 44:476–479. [PubMed: 12939068]
8. Bley CR, Blattmann H, Roos M, et al. Assessment of a radiotherapy patient immobilization device using single plane radiographs and a remote computed tomography scanner. Vet Radiol Ultrasound. 2003; 44:470–475. [PubMed: 12939067]
9. Lawrence JA, Forrest LJ, Turek MM, et al. Proof of principle of ocular sparing in dogs with sinonasal tumors treated with intensity-modulated radiation therapy. Vet Radiol Ultrasound. 2010; 51:561–570. [PubMed: 20973393]
10. Forrest LJ, Mackie TR, Ruchala K, et al. The utility of megavoltage computed tomography images from a helical tomotherapy system for set-up verification purposes. Int J Radiat Oncol Biol Phys. 2004; 60:1639–1644. [PubMed: 15590196]
11. Yan JH, Xu GZ, Hu YH, et al. Management of local residual primary lesion of nasopharyngeal carcinoma: II. Results of prospective randomized trail on booster dose. Int J Radiat Oncol Biol Phys. 1990; 18:295–298. [PubMed: 2406228]
12. Yan D, Wong J, Vicini F, et al. Adaptive modification of treatment planning to minimize the deleterious effects of treatment setup errors. Int J Radiat Oncol Biol Phys. 1997; 38:197–206. [PubMed: 9212024]

13. Van Herk M, Remeijer P, Rasch C, et al. The probability of correct target dosage: Dose-population histograms for deriving treatment margins in radiotherapy. Int J Radiat Oncol Biol Phys. 2000; 47:1121–1135. [PubMed: 10863086]
14. Prescribing, Recording and Reporting Photon Beam Therapy, Report 62. International Commission on Radiation Units and Measurements (ICRU). 1999
15. Hong TS, Tome WA, Chappell RJ, Chinnaiyan P, Mehta MP, Harari PM. The impact of daily setup variations on head-and-neck intensity modulated radiation therapy. Int J Radiat Oncol Biol Phys. 2005; 61:779–788. [PubMed: 15708257]
16. Hunt MA, Kutcher GJ, Burman C, et al. The effect of setup uncertainties on the treatment of nasopharynx cancer. Int J Radiat Oncol Biol Phys. 1993; 27:437–447. [PubMed: 8407420]
17. Siebers JV, Lauterbach M, Keall PJ, et al. Incorporating multileaf collimator leaf sequencing into iterative IMRT optimization. Med Phys. 2002; 29:952–959. [PubMed: 12094990]
18. Manning MA, Wu Q, Cardinale RM, et al. The effect of setup uncertainty on normal tissue sparing with IMRT for head-and-neck cancer. Int J Radiat Oncol Biol Phys. 2001; 51:1400–1409. [PubMed: 11728701]
19. Deveau MA, Gutierrez AN, Mackie TR, et al. Dosimetric impact of daily setup variations during treatment of canine nasal tumors using intensity-modulated radiation therapy. Vet Radiol Ultrasound. 2010; 51:90–96. [PubMed: 20166402]
20. Bunting, LN.; Deveau, M.; Forrest, LJ. Proceedings of the 30th Veterinary Cancer Society Conference; October 30, 2011; San Diego, CA. p. 47
21. Kippenes H, Gavin PR, Sande RD, et al. Comparison of the accuracy of positioning devices for radiation therapy of canine and feline head tumors. Vet Radiol Ultrasound. 2000; 41:371–376. [PubMed: 10955503]

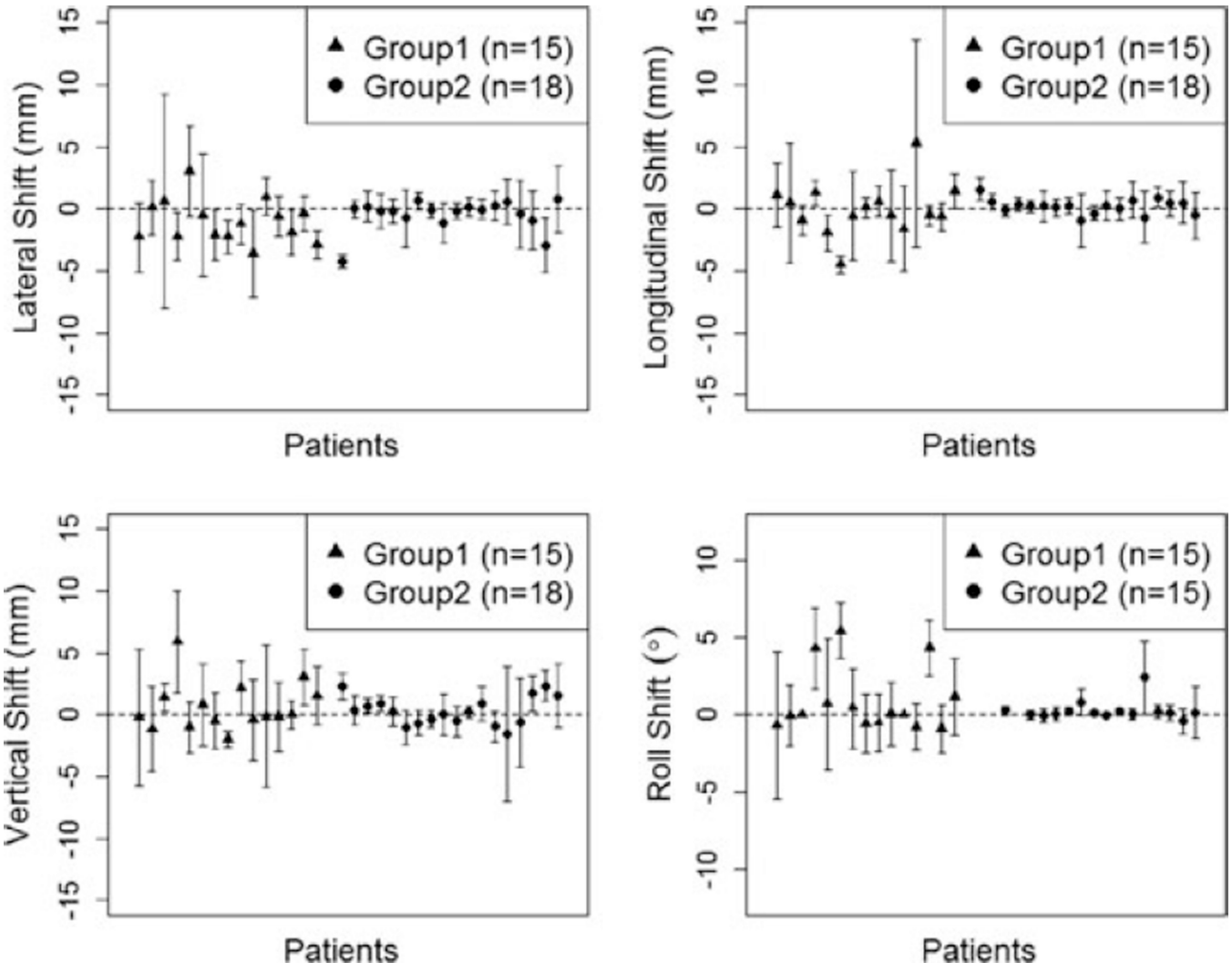

Fig. 1.
Mean (± standard deviation) setup correction for each individual patient.

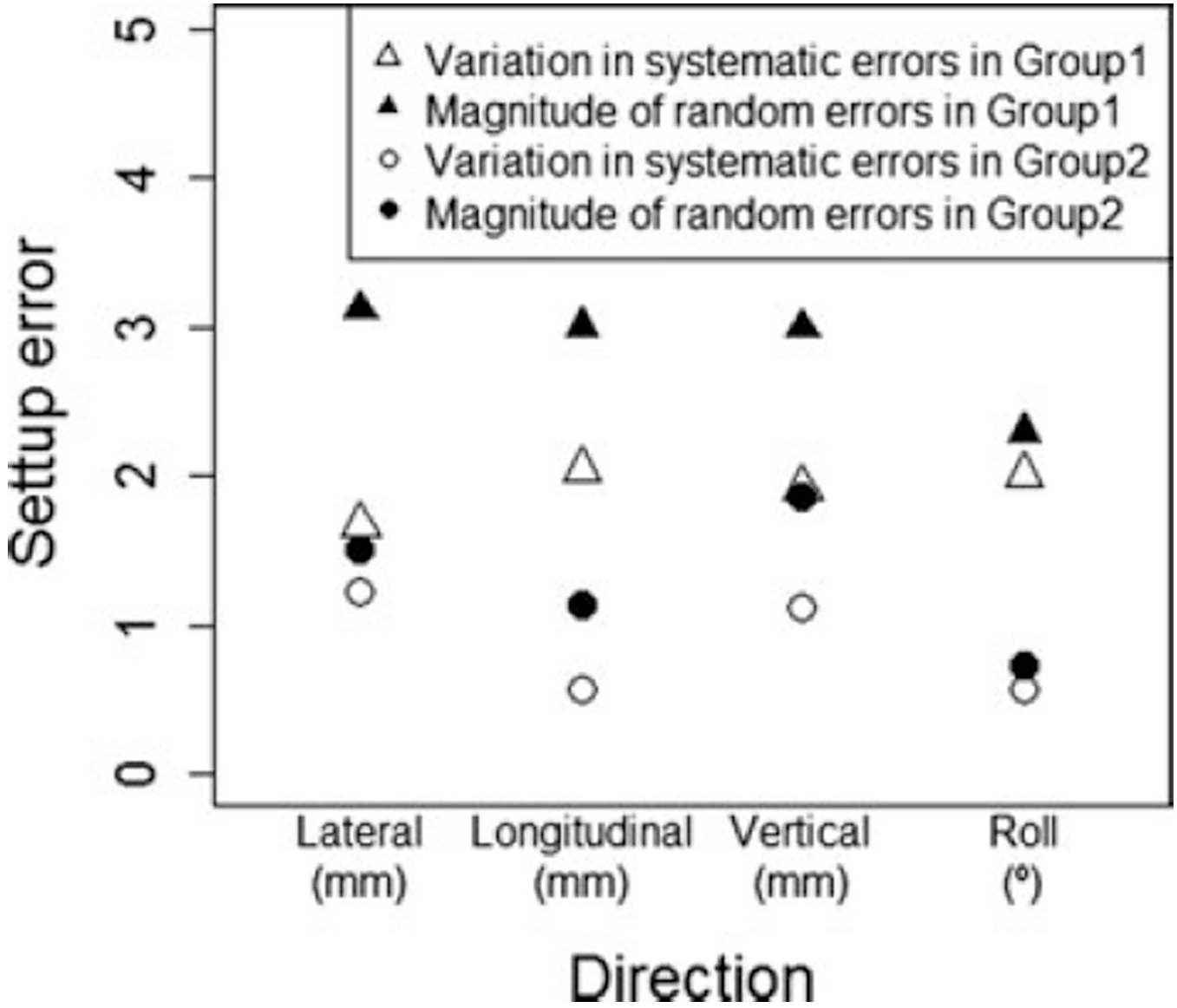

Fig. 2.
Setup errors.

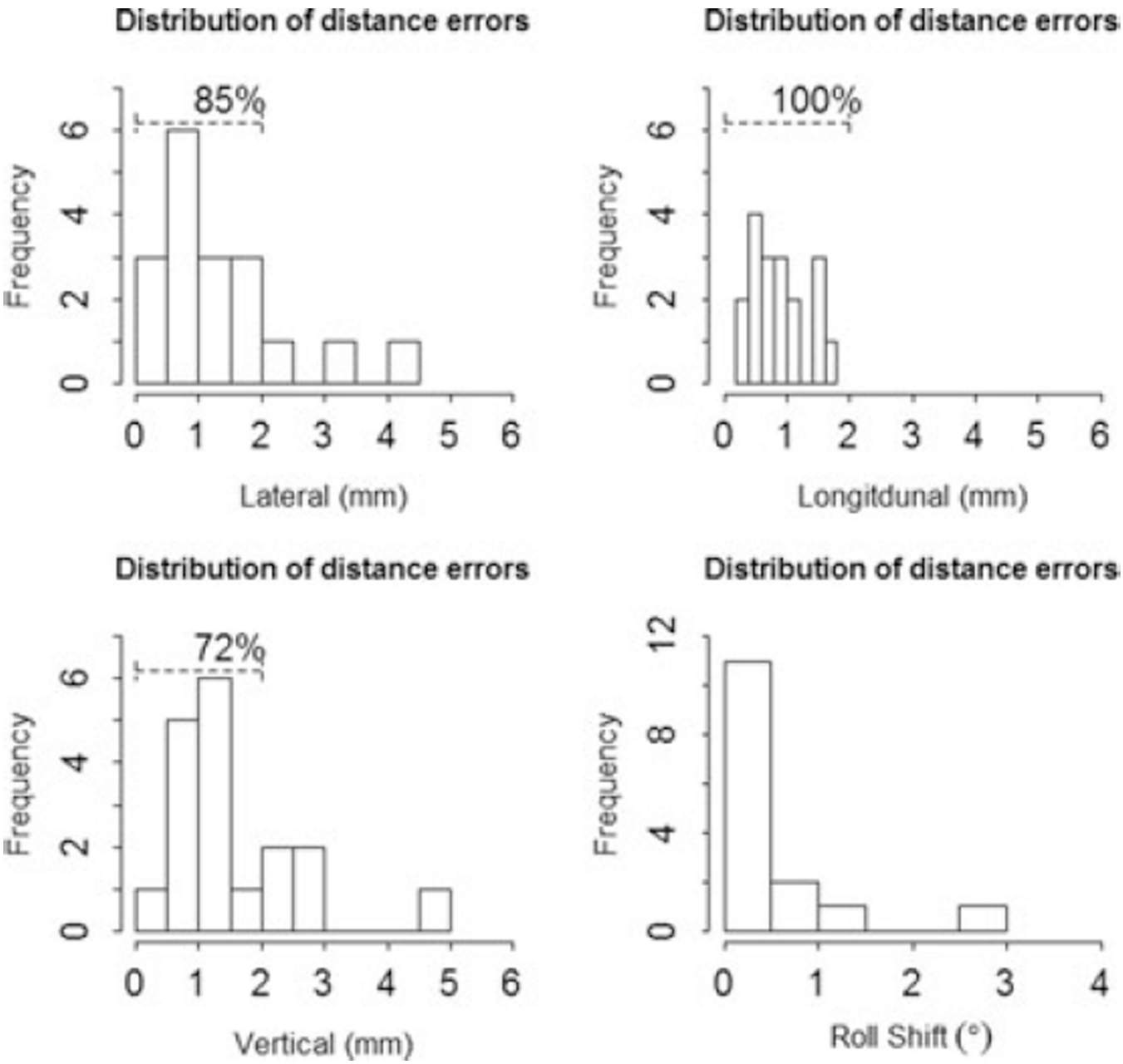

Fig. 3.
Distribution of distance errors.

Photograph 1.
Patient immobilized in bite block

Table 1

Comparison of the systematic errors between the two groups

Direction of the measurements		Group 1 (n = 15)	Group 2 (n = 18)	P-value*
Lateral (mm)	Mean	−1.02	−0.47	0.15
	Median	−1.21	−0.13	
	Std	1.73	1.26	
	Min	−3.57	−4.24	
	Max	3.04	0.79	
Longitudinal (mm)	Mean	−0.06	0.2	0.46
	Median	−0.5	0.23	
	Std	2.11	0.6	
	Min	−4.53	−0.95	
	Max	5.3	1.56	
Vertical (mm)	Mean	0.61	0.3	1
	Median	−0.15	0.23	
	Std	1.98	1.15	
	Min	−1.99	−1.58	
	Max	5.87	2.34	
Roll (°)†	Mean	0.85	0.27	0.56
	Median	0.01	0.13	
	Std	2.07	0.64	
	Min	−0.91	−0.41	
	Max	5.42	2.42	

*Wilcoxon rank sum test.

†Three patients were missing in Group 2 (n = 15).

Table 2

Comparison of the random errors between the two groups

Direction of the measurements		Group 1 (n = 15)	Group 2 (n = 18)	P-value*
Lateral (mm)	Mean	2.67	1.4	0.01
	Median	1.93	1.19	
	Std	1.96	0.77	
	Min	1.1	0.57	
	Max	8.63	2.74	
Longitudinal (mm)	Mean	2.41	1.07	0.02
	Median	1.39	0.9	
	Std	2.1	0.55	
	Min	0.7	0.47	
	Max	8.37	2.14	
Vertical (mm)	Mean	2.8	1.55	<0.01
	Median	2.36	1.21	
	Std	1.47	1.22	
	Min	0.68	0.45	
	Max	5.72	5.47	
Roll (°)†	Mean	2.08	0.6	<0.01
	Median	1.88	0.41	
	Std	1.26	0.62	
	Min	0	0.09	
	Max	4.75	2.36	

*Wilcoxon rank sum test.

†Three patients were missing in the Group 2 (n = 15).

Table 3

Variation in systematic errors and magnitude of random errors

Direction of the measurements		Variation in systematic errors	Magnitude of random errors (RMS)
Lateral	Group 1 (n = 15)	1.68	3.12
	Group2 (n = 18)	1.23	1.51
Longitudinal	Group 1 (n = 15)	2.05	3
	Group 2 (n = 18)	0.58	1.14
Vertical	Group 1 (n = 15)	1.92	2.99
	Group 2 (n = 18)	1.12	1.86
Roll *	Group 1 (n = 15)	2.01	2.29
	Group 2 (n = 15)	0.57	0.74

* Three patients were missing in the Group 2 (n = 15).

Table 4

Comparison of the distance errors between the two groups

Direction of the measurements		Group 1 (n = 15)	Group 2 (n = 18)	P-value*
Lateral (mm)	Mean	2.57	1.35	<0.01
	Median	2.46	1.01	
	Std	1.2	1.01	
	Min	1	0.42	
	Max	5.4	4.24	
Longitudinal (mm)	Mean	2.38	0.91	<0.01
	Median	1.75	0.81	
	Std	2.05	0.43	
	Min	0.5	0.37	
	Max	8.28	1.77	
Vertical (mm)	Mean	2.68	1.59	<0.01
	Median	2.42	1.31	
	Std	1.32	1.02	
	Min	0.78	0.43	
	Max	5.95	4.56	
Roll (°)†	Mean	2.15	0.5	<0.01
	Median	1.77	0.26	
	Std	1.6	0.64	
	Min	0	0.05	
	Max	5.42	2.62	

*Wilcoxon rank sum test.

†Three patients were missing in Group 2 (n = 15).

Table 5

Comparison of the variation of setup corrections from the zero shift between the two groups

Direction of the measurements		Group 1 (n = 15)	Group 2 (n = 18)	P-value*
Lateral (mm)	Mean	3.25	1.7	<0.01
	Median	2.84	1.27	
	Std	1.77	1.09	
	Min	1.41	0.55	
	Max	8.21	4.27	
Longitudinal (mm)	Mean	2.91	1.17	<0.01
	Median	2.37	1.1	
	Std	2.23	0.57	
	Min	0.77	0.46	
	Max	9.55	2.24	
Vertical (mm)	Mean	3.26	1.85	<0.01
	Median	2.98	1.54	
	Std	1.58	1.19	
	Min	1.05	0.47	
	Max	7.07	5.42	
Roll (°)†	Mean	2.67	0.7	<0.01
	Median	1.96	0.39	
	Std	1.74	0.82	
	Min	0	0.08	
	Max	5.68	3.3	

*Wilcoxon rank sum test.

†Three patients were missing in Group 2 (n = 15).